*4800–4807* *Nucleic Acids Research, 2001, Vol. 29, No. 23* 

# A mRNA-based thermosensor controls expression of rhizobial heat shock genes

**Andreas Nocker, Thomas Hausherr, Sylvia Balsiger, Nila-Pia Krstulovic, Hauke Hennecke and Franz Narberhaus***

Institut für Mikrobiologie, Eidgenössische Technische Hochschule, Schmelzbergstrasse 7, CH-8092 Zürich, Switzerland

Received August 23, 2001; Revised and Accepted October 8, 2001

## ABSTRACT

**Expression of several heat shock operons, mainly coding for small heat shock proteins, is under the control of ROSE (repression of heat shock gene expression) in various rhizobial species. This negatively *cis*-acting element confers temperature control by preventing expression at physiological temperatures. We provide evidence that ROSE-mediated regulation occurs at the post-transcriptional level. A detailed mutational analysis of $ROSE_1$–*hspA* translationally fused to *lacZ* revealed that its highly conserved 3′-half is required for repression at normal temperatures (30°C). The mRNA in this region is predicted to form an extended secondary structure that looks very similar in all 15 known ROSE elements. Nucleotides involved in base pairing are strongly conserved, whereas nucleotides in loop regions are more divergent. Base substitutions leading to derepression of the *lacZ* fusion at 30°C exclusively resided in potential stem structures. Optimised base pairing by elimination of a bulged residue and by introduction of complementary nucleotides in internal loops resulted in ROSE elements that were tightly repressed not only at normal but also at heat shock temperatures. We propose a model in which the temperature-regulated secondary structure of ROSE mRNA influences heat shock gene expression by controlling ribosome access to the ribosome-binding site.**

## INTRODUCTION

When cells are exposed to a sudden temperature upshift, a set of highly specialized proteins is induced. The family of so-called heat shock proteins (Hsps) is comprised of molecular chaperones (e.g. DnaK and GroEL) and proteases (e.g. Lon, Clp, FtsH and DegP) which play important roles in modulating protein folding, refolding of denatured proteins and their degradation (1). Despite the universality of the heat shock response, the mechanisms controlling expression of these proteins vary substantially even within the same organism. Bacteria use at least two strategies to control heat shock gene expression involving positive and negative regulatory principles.

Positive regulation is based on specific recognition of heat shock gene promoters by alternative σ factors, up-regulating expression of the corresponding regulon. The currently best-studied heat shock σ factor is $\sigma^{32}$ (RpoH) of *Escherichia coli*. A sudden temperature upshift leads to accumulation of $\sigma^{32}$. This results in induction of about 30 $\sigma^{32}$-controlled heat shock genes (2). The up-regulation of $\sigma^{32}$ is mainly caused by enhanced translation of *rpoH* mRNA (see Discussion) and by the increased activity and stability of its product. The σ factor is subject to feedback control by the DnaK machinery, consisting of DnaK, DnaJ and GrpE, which sequesters $\sigma^{32}$ under non-stress conditions (activity control) and is also responsible for its rapid turnover by promoting degradation by the FtsH protease (stability control). In the presence of unfolded proteins after heat shock, DnaK is presumably titrated away from $\sigma^{32}$. The σ factor can then associate with RNA polymerase core enzyme and induce transcription of the $\sigma^{32}$ regulon (1–3).

Negative regulation of heat shock genes depends on specific binding of a repressor protein to a target sequence in the promoter region (4). This mechanism allows temperature control of heat shock genes preceded by vegetative promoters. Upon heat shock, the protein–DNA interaction is abolished, leading to induction of transcription. One of the most widely distributed negative heat shock control mechanisms is the CIRCE system (controlling inverted repeat of chaperone expression) (5). The presence of this negatively *cis*-acting DNA element has been documented in more than 70 operons of some 40 Eubacteria (4,6,7). CIRCE is believed to function both as a binding site for the repressor protein HrcA (heat regulation at CIRCE) (8) and in promoting rapid mRNA turnover under normal conditions by forming a destabilizing mRNA secondary structure (9,10). Thus, regulation occurs at the transcriptional and post-transcriptional levels. HrcA depends on GroESL to acquire an active inhibitory conformation. Depletion of the GroE pool by denatured proteins after a heat shock presumably renders HrcA inactive and thus results in elevated expression of CIRCE-controlled heat shock genes (11,12). Other examples for negative heat shock control are the HspR regulon of *Streptomycetes*, the CtsR regulon of *Bacillus subtilis* and RheA (OrfY) of *Streptomyces albus* (4,13). The latter was shown to act as a direct thermosensor. A reversible temperature-dependent conformational change is responsible

*To whom correspondence should be addressed. Tel: +41 1 632 2586; Fax: +41 1 632 1148; Email: fnarber@micro.biol.ethz.ch

for the transition from an active DNA-binding to an inactive form (14).

The heat shock response of *Bradyrhizobium japonicum*, the nitrogen-fixing root nodule symbiont of soybean, is controlled by a complex network involving a combination of both positive (e.g. RpoH; 15) and negative (e.g. CIRCE; 16) regulatory principles. At least five heat shock operons, however, are under the control of a new type of regulatory element called ROSE (repression of heat shock gene expression), a conserved DNA segment of ~100 bp, which is positioned in the 5′-untranslated region (5′-UTR) precisely between the transcriptional and translational start sites (17,18). This *cis*-acting element mainly regulates genes that encode small heat shock proteins (sHsps), but also controls $rpoH_1$ coding for one of three *B.japonicum* $\sigma^{32}$ factors. ROSE elements have recently been identified in three other rhizobia, namely in *Bradyrhizobium* sp. (*Parasponia*), *Rhizobium* sp. strain NGR234 and *Mesorhizobium loti* (19). The elements are functionally interchangeable among the species. Internal deletions in ROSE resulted in derepressed transcript levels and in elevated β-galactosidase activities of translational $ROSE_1$–*hspA*–lacZ fusions (17). On the basis of the retardation of a $ROSE_1$ fragment by an unknown protein in crude extracts from *B.japonicum* grown at 30°C, it was speculated initially that regulation depends on specific binding of a repressor protein. However, three independent strategies that were applied to identify the cognate ROSE-binding protein failed: (i) purification of the putative binding protein; (ii) transposon mutagenesis of a *B.japonicum* $ROSE_1$–*hspA*–*lacZ* reporter strain; (iii) transformation of an *E.coli* host strain bearing the same reporter with *B.japonicum* gene banks (A.Nocker, unpublished results).

The goal of this study was to evolve an alternative model of how ROSE might control the expression of heat shock genes. We present the identification of a functionally important segment at the promoter-distal end of ROSE and propose a novel mechanism of post-transcriptional heat shock regulation.

## MATERIALS AND METHODS

### Bacterial strains, plasmids and growth conditions

*Escherichia coli* strains were grown in Luria–Bertani medium at 37°C (for cloning purposes) or 30°C (for mutant screening and β-galactosidase assays if not mentioned otherwise). *Bradyrhizobium japonicum* strains were propagated aerobically at 30°C in PSY medium (20) supplemented with 0.1% (w/v) arabinose. If appropriate, antibiotics were added in the following final concentrations: spectinomycin, 100 μg/ml; chloramphenicol, 30 μg/ml (for counterselection against *E.coli* donor strains); tetracycline, 10 μg/ml (*E.coli* strains) or 50 μg/ml (*B.japonicum* strains).

### DNA manipulations and sequence analysis

Standard protocols were used for recombinant DNA techniques (21). Multiple sequence alignments were generated using CLUSTAL W (22) before they were imported into the multiple sequence alignment editor and shading utility GeneDoc (www.psc.edu/biomed/genedoc). RNA secondary structures were predicted with the mfold program (v.3.1) provided by Zuker *et al.* (23) on the Internet (http://www.bioinfo.math.rpi.edu/~mfold/rna).

### Construction of plasmids and strains

All plasmids were constructed in *E.coli* DH5α (Bethesda Research Laboratories). $ROSE_1$-carrying inserts for translational fusions originated either from random or from site-directed mutagenesis. Plasmid pRJ5064, which contains a 718 bp *Pst*I fragment carrying $ROSE_1$ (102 bp) flanked by a 264 bp upstream sequence and the 5′-end (352 bp) of *hspA* was used (17). Random mutagenesis was performed by error-prone PCR using *Taq* DNA polymerase and various modifications to the standard protocol, which are known to favor misincorporation of nucleotides (Table 1). The entire insert of pRJ5064 was amplified using primers AN19 (5′-TCGACCCCGGGAACATCGCCAAAGGCTCAC-3′, introduced *Sma*I site underlined) and AN20 (5′-CTTGGCTGCAGCAAGCCGTTG-3′, introduced *Pst*I site underlined). PCR products were digested with *Sma*I and *Pst*I and used to replace the $ROSE_1$–*hspA* fragment in pRJ5400, a pSUP derivative that carries a translational $ROSE_1$–*hspA*–*lacZ* fusion (17). The plasmid pool was mobilized from *E.coli* S17-1 (24) into *B.japonicum* 110*spc*4 for genomic integration (20). Derepressed $ROSE_1$ variants from colonies that turned blue on plates containing Xgal were amplified by colony PCR and sequenced.

Site-directed mutagenesis was performed according to the instruction manual of the QuikChange mutagenesis kit (Stratagene). Plasmid pRJ5064 served as template. Mutagenic primers and the resulting $ROSE_1$ mutations are listed in Table 2. The inserts containing mutated $ROSE_1$ variants were isolated upon *Pst*I digestion and subcloned into the corresponding site upstream of *lacZ* of pSUP482 (16). The $_2CC_3 \rightarrow AG$ mutation was constructed using tail-to-tail primers (25) in order to introduce a *Xho*I restriction site immediately downstream of the transcription start site of $ROSE_1$–*hspA*. Before integration into *B.japonicum* 110*spc*4, the sequences of all mutated ROSE elements were confirmed by automated sequencing.

### β-Galactosidase assay

If not mentioned otherwise, *B.japonicum* and *E.coli* strains were grown aerobically at 30°C in the appropriate medium to a cell density of ~0.5 at $A_{600}$. β-Galactosidase assays were performed as described previously (19).

### Transcript mapping

RNA isolation and primer extension analyses were performed as described elsewhere (11). Primer extensions with total RNA were carried out with oligonucleotide Sig107 (TCTACATTGCAGGGTGGGTAGTTGGCTTC), whose 5′-end is equivalent to position 224 in the *hspA* gene.

## RESULTS

### Highly similar potential secondary structures in ROSE mRNAs

Comparative analyses of expression from a number of transcriptional and translational *lacZ* fusions to ROSE demonstrated that proper heat regulation occurred only in the context of translational fusions (data not shown). In variance

**Table 1.** Single nucleotide exchanges in $ROSE_1$ obtained by error-prone PCR mutagenesis

| Mutation in $ROSE_1$ | PCR conditions |
|---|---|
| A10G | Two PCR reactions: first with 7.5 mM $MgCl_2$; second with an aliquot of the first reaction in 5 mM $MgCl_2$ |
| G55A | See above |
| C59T | 5 mM $MgCl_2$ |
| C71T | Two PCR reactions: (i) four parallel reactions each with 1.6 mM (8-fold excess) of one nucleotide; (ii) aliquot of pooled first reaction with 5 mM $MgCl_2$ |
| T77C | Standard conditions (2.5 mM $MgCl_2$) |
| T79C | See above |
| T85C | Four parallel reactions each with 1.6 mM (8-fold excess) of one nucleotide |
| T98A | 0.2 mM $MnCl_2$ |
| A106T | 0.2 mM $MnCl_2$ |

with earlier assumptions, this strongly suggested regulation by ROSE at the post-transcriptional level. We speculated that this might be due to the formation of secondary structures in the extended 5′-UTR.

To gain insight into potential secondary structures of ROSE mRNAs, we applied the latest mfold program by Zuker and Turner (see Materials and Methods). All ROSE elements adopt secondary structures, as exemplified for representative ROSE elements of different lengths from four different rhizobial species (Fig. 1A–D). The promoter-proximal structures varied from element to element. Even in one given ROSE element several alternative folding options were predicted in the 5′-region (data not shown).

Most strikingly, the folding pattern of the 3′-end of all ROSE elements (marked by frames) was highly similar in all cases (Figs. 1A–D). Stem formation was always interrupted by one or more short unpaired regions and by a bulged G residue opposite the Shine–Dalgarno (SD) sequence. In each case, the SD sequence and the translational start codon were engaged in base pairing. Interestingly, the predicted structures in the 3′-end coincide with a highly conserved region of all 15 known ROSE elements (Fig. 1E), lending support to the idea that this region might be of functional relevance (19). From the alignment of that region of all 11 ROSE elements functionally characterized to date it is evident that those $ROSE_1$ residues that contribute to base pairing (indicated by blue bars) are highly conserved, whereas potential loop regions are not.

## Nucleotides in the 3′-half of ROSE are required for repression

To pinpoint individual nucleotides in $ROSE_1$ important for repression, we used two complementary strategies. First, a fragment containing the regulatory element was subjected to error-prone PCR amplification before translational *hspA–lacZ* fusions were constructed (Fig. 2A). Many constructs obtained carried more than one nucleotide exchange. Only those containing a single mutation in the ROSE region were examined further (Table 1). Secondly, rationally designed mutated ROSE fragments were produced (Table 2) and cloned in-frame with the *lacZ* gene. All ROSE variants were chromosomally integrated into

**Table 2.** Construction of site-directed $ROSE_1$ variants

| Mutated sequence in $ROSE_1$ | Mutagenic primers | Primer sequences [a] |
|---|---|---|
| CCGG(16-19)AATT | AN39 | CCGCGACAAGCGGTAATTGCGCCCTAGGGGCCCGGCGG |
| | AN40 | GGCCCCTAGGGCGCAATTACCGCTTGTCGCGGCGAGCAG |
| GACG(41-44)TTAT | AN26 | GGGGCCCGGCGGATTATGGCGCCGGAGGTGTCCGACG |
| | AN27 | CACCTCCGGCGCCATAATCCGCCGGGCCCCTAGGGCG |
| CGGA(50-53)ATTC, | AN47 | CGGAGACGGGCGCATTCGGTGGAATACGCCTGCTCG |
| TCCG(58-61)GAAT | AN48 | GGCGTATTCCACCGAATGCGCCCGTCTCCGCCGGGC |
| TCCG(58-61)GAAT | AN28 | GCGCCGGAGGTGGAATACGCCTGCTCGTACCCATC |
| | AN29 | ACGAGCAGGCGTATTCCACCTCCGGCGCCCGTCTC |
| CGCC(63-66)ATAA | AN24 | CGGAGGTGTCCGAATAATGCTCGTACCCATCTTGC |
| | AN25 | GATGGGTACGAGCATTATTCGGACACCTCCGGCGC |
| TA(73,74)CG | AN41 | CGACGCCTGCTCGVBCCCATCTTGCTCCTTGGAG |
| | AN42 | GGAGCAAGATGGGVBCGAGCAGGCGTCGGACACC |
| TT(81,82)GG | AN35 | GCTCGTACCCATCNVGCTCCTTGGAGGATTTGG |
| TT(81,82)GA | AN36 | TCCTCCAAGGAGCBNGATGGGTACGAGCAGGC |
| T82A | | |
| G83Δ | Sig191 | TCGTACCCATCTTΔCTCCTTGGAGGATTTGG |
| | Sig192 | TCCTCCAAGGAGΔAAGATGGGTACGAGCAG |
| G83A | Sig193 | TCGTACCCATCTTACTCCTTGGAGGATTTGG |
| | Sig194 | TCCTCCAAGGAGTAAGATGGGTACGAGCAG |
| G83A, C80A, U79A, C75G | Sig195 | CTGCTCGTAGCCAAATTACTCCTTGGAGGATTTGG |
| ('tight stem') | Sig196 | TCCTCCAAGGAGAAATTTGGCTACGAGCAGGCGTCG |
| C84A | AN45 | GTACCCATCTTGDTCCTTGGAGGATTTGG |
| C84G | AN46 | ATCCTCCAAGGAHCAAGATGGGTACGAGC |
| C84T | | |
| A109C | AN43 | TGGCTATGAGGBCTTACAACATCAGCC |
| A109G | AN44 | GATGTTGTAAGVCCTCATAGCCAAATC |

[a]Mutated positions are underlined. The letters B, D, H, N and V correspond to the IUPAC code for mixed bases: B = C, G or T; D = A, G or T; H = A, C or T; N = A, C, G or T; V = A, C or G).

*B.japonicum*. The identical low copy number plasmids used for conjugation were also examined in *E.coli* DH5α in order to check for potential ROSE-regulated expression in this background. The β-galactosidase activities at 30°C of blue colonies selected from the random mutagenesis approach and of site-directed ROSE variants were determined in both strains. The relative expression in comparison with Bj5400 and Ec5400 carrying the $ROSE_1^{WT}$ fusion (17) is depicted in Figure 2B and C.

The mutational analysis shows that several single nucleotide exchanges are sufficient to permit *hspA* expression even at low temperatures. Interestingly, almost all mutations responsible for derepression were located in the promoter-distal end of ROSE (Fig. 2B). One mutation (A106→T) leading to high expression at 30°C is even located in the coding sequence of the *hspA* gene. These results are in perfect agreement with results obtained by the analysis of insertions and deletions in ROSE (17). Nucleotides whose exchange resulted in derepression in the present work clustered in or downstream of a region (50–102) previously found to be important. Moreover, the random mutagenesis approach did not reveal any critical nucleotides in the region 22–47, whose deletion had been found to leave *hspA* expression unaffected.

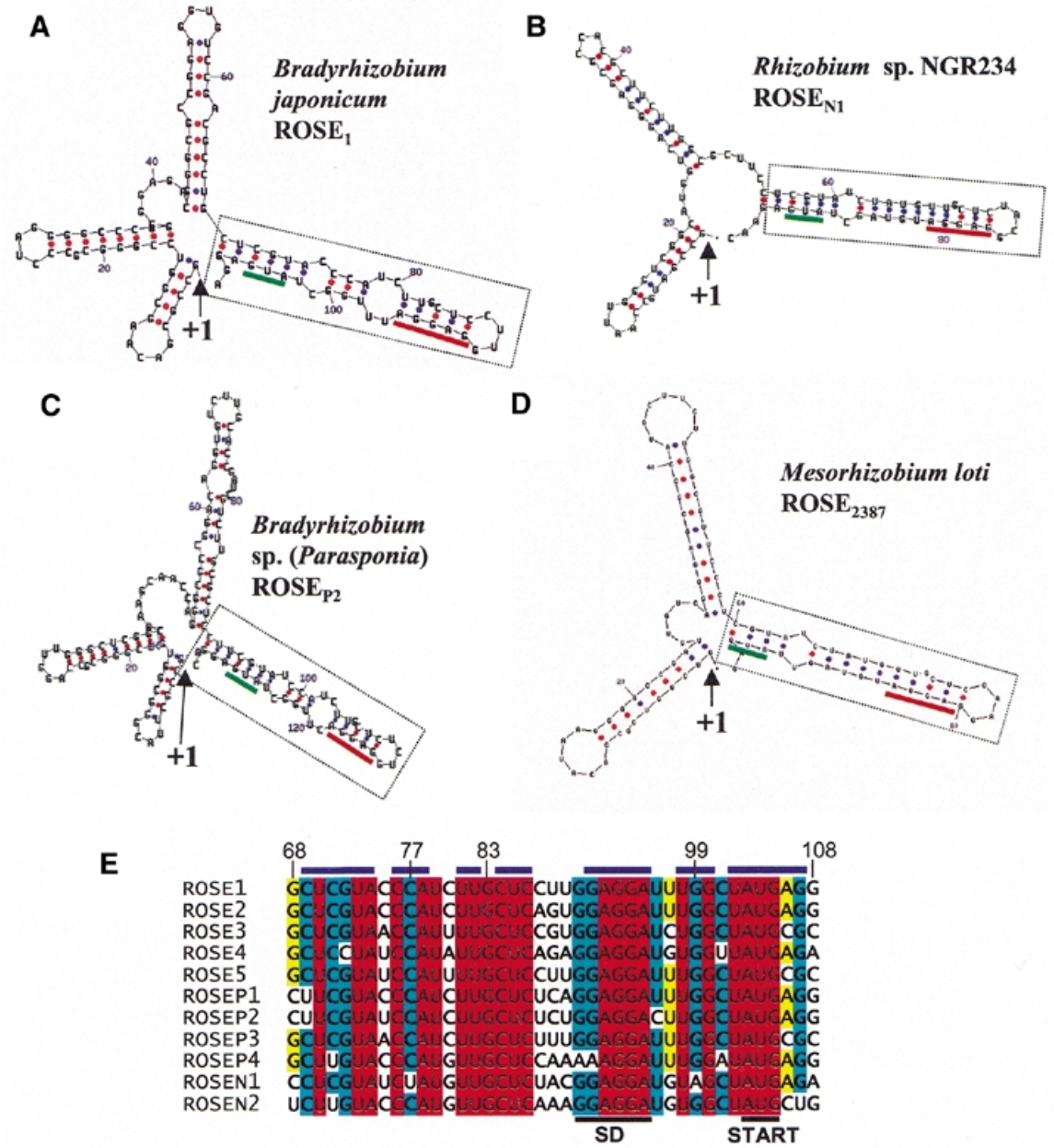


**Figure 1.** Secondary structure predictions of ROSE mRNAs from different rhizobia and sequence alignment of the conserved 3′-regions of 11 previously characterized ROSE elements. (**A**–**D**) Predicted mRNA structures of $ROSE_1$ from *B.japonicum*, $ROSE_{P2}$ from *Bradyrhizobium* sp. (*Parasponia*), $ROSE_{N1}$ from *Rhizobium* sp. NGR234 and *M.loti* $ROSE_{2387}$, respectively. Nucleotides are numbered starting from the transcription start site at +1. Each sequence comprises the entire ROSE element including the SD sequence (underlined in red), the translation start site (AUG, underlined in green) and a few additional nucleotides of the coding region. Red dots indicate C-G pairs and blue dots either U-A or U-G pairs. Highly similar structures formed by the 3′-halves of all ROSE elements are marked by a rectangular frame. (**E**) Alignment of the 3′-ends of ROSE mRNAs from *B.japonicum* ($ROSE_{1–5}$), *Bradyrhizobium* sp. (*Parasponia*) ($ROSE_{P1–P4}$) and *Rhizobium* sp. NGR234 ($ROSE_{N1, N2}$). Conserved nucleotides are highlighted as follows: red, conserved in all 11 elements; light blue, conserved in at least nine elements; yellow, conserved in at least seven elements. Residues relevant for the Discussion section, the SD sequence and the translation start sites (START) are indicated. Blue lines on top of the alignment mark $ROSE_1$ regions involved in base pairing.

Derepression in *B.japonicum* was reflected in elevated transcript levels, as shown by primer extension analysis for the two most strongly inducing mutations $_{81}TT_{82}$→GA and C84→A. The *hspA* transcript levels at 30°C of these mutants were almost as high as in heat-shocked cells carrying wild-type $ROSE_1$ (Fig. 3, lanes 3–5).

Interestingly, ROSE-mediated regulation was also observed in the *E.coli* background (Fig. 2C). Although the induction factors were generally lower, it is important to note that similar nucleotides were found to be critical for repression in both organisms. The only major difference concerned two highly conserved positions immediately downstream of the transcription start site. These nucleotides seem to be important only in *B.japonicum*. The reason for this discrepancy presumably lies in the fact that transcription in *E.coli* did not initiate from the *hspA* promoter upstream of $ROSE_1$ but from undefined positions

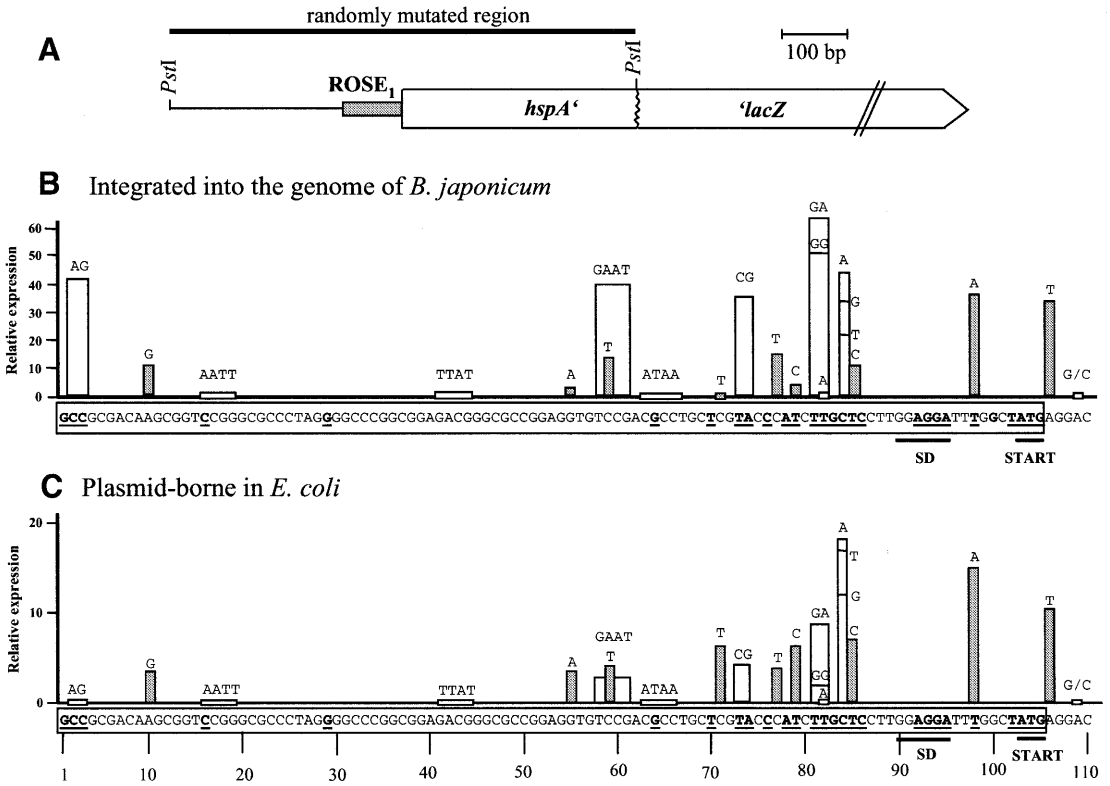


**Figure 2.** Effect of point mutations in translational ROSE$_1$–*hspA*–*lacZ* fusions. (**A**) Schematic representation of the translational ROSE$_1$–*hspA*–*lacZ* fusion used for error-prone mutagenesis and for construction of site-directed mutants in ROSE$_1$. (**B** and **C**) Effect of base substitutions on the expression of ROSE$_1$–*hspA*–*lacZ* fusions that were either integrated into the genome of *B.japonicum* (B) or plasmid-borne in *E.coli* DH5α (C). The DNA sequence of ROSE is shown. Nucleotides conserved in all 11 experimentally characterized elements are marked by underlined bold letters. (B) and (C) show the relative β-galactosidase activity of those ROSE versions listed in Tables 1 and 2 that were generated either by random PCR (grey columns) of the *Pst*I fragment indicated in (A) or by site-directed mutagenesis (white columns). Relative expression is the ratio of β-galactosidase activity between strains carrying base substitutions in ROSE$_1$–*hspA* and the host strain Bj5400 (B) or Ec5400 (C) carrying the wild-type ROSE$_1$–*hspA* fragment. The β-galactosidase values of Bj5400 and Ec5400 were ~1.0 and 2.7 MU, respectively. All values were obtained from between two and four independent cultures with a standard deviation of ~20%.

in the pSUP vector, as demonstrated by primer extension analysis (data not shown). *In vitro* transcription experiments confirmed that *E.coli* RNA polymerase is unable to recognize the *hspA* promoter (data not shown).

### Base pairing is essential for repression

The predicted mRNA hairpin at the 3′-end of ROSE$_1$, boxed in Figure 1A, is magnified in Figure 4. Three complimentary stretches are interrupted by two internal loops and one peripheral loop. The SD sequence and the translational start codon are located in the first and third paired region, respectively. Most importantly, those nucleotides whose exchange abrogated ROSE-mediated repression (Fig. 2B and C) are all involved in base pairing (red asterisks in Fig. 4). On the other hand, nucleotides that could be exchanged without altering expression levels (green rectangles) or that are variable between ROSE elements (blue triangles) resided in loop regions. The exception, a paired C at position 71, could be replaced by a U without any effect, presumably because base pairing with the opposite G was sustained. Hence, the combination of our mutational analysis and the structure predictions strongly suggest that post-transcriptional regulation by ROSE involves the formation of folded mRNA species.

### Removal of a bulged residue opposite the SD sequence enhances repression

Next we asked whether the opposite strategy, namely stabilization of the putative hairpin, would further strengthen repression by ROSE at normal temperatures and reduce induction at heat shock temperatures. An obvious candidate for this approach is G83, an invariant nucleotide in all known ROSE elements (Fig. 1E) that is located as a bulged residue opposite the SD sequence (Fig. 4). Experiments were initially performed in *E.coli* because in this organism β-galactosidase expression can be monitored at elevated temperatures, whereas *B.japonicum* will not grow at temperatures higher than 34°C. When *E.coli* carrying pRJ5400 with the wild-type ROSE$_1$–*hspA*–*lacZ* fusion was grown at 30°C, the β-galactosidase activity was 2.1 Miller units (MU). At 37°C, expression was elevated ~10-fold to 23.3 MU (Fig. 5). The replacement of G83 by an adenine (G83→A) did not change expression levels. On the other hand, eliminating G83 in G83Δ had two important consequences. First, β-galactosidase activity at repressing temperatures (30°C) was further decreased ~2-fold to 1.1 MU. Secondly, expression was not derepressed at 37°C. The same lack of temperature responsiveness was observed when no internal bulges or loops were allowed in the 3′-end of ROSE (G83Δ,

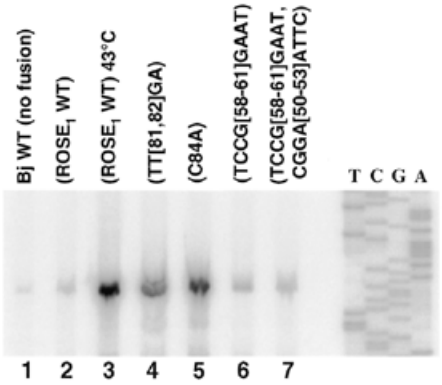


**Figure 3.** Effect of ROSE mutations on transcription. Primer extension experiments were carried out with total RNA from wild-type *B.japonicum* (WT) or from strains with a co-integrated translational ROSE$_1$–*hspA*–*lacZ* fusion. Base substitutions in ROSE$_1$ are indicated in brackets. All cells were grown at 30°C. A sample of the Bj5400 culture was subjected to heat shock for 30 min at 43°C (lane 3). Both the reverse transcription and the sequencing reaction (TCGA, pRJ5400 as template) were performed with primer Sig107.

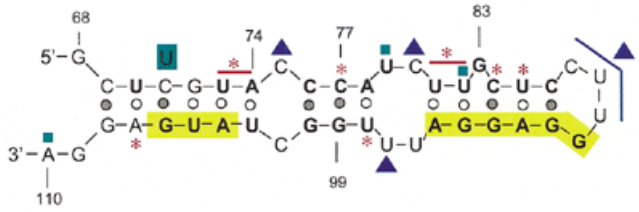


**Figure 4.** Effect of ROSE$_1$ mutations on the mRNA structure at the 3′-end. Numbers represent the nucleotide positions relative to the transcription start site. Conserved nucleotides are indicated in bold. The translation start site and the SD sequence are highlighted in yellow. White circles symbolize base pairing through two hydrogen bonds, grey circles base pairing between C and G through three hydrogen bonds. Exchange of nucleotides marked with a red asterisk led to derepression of the corresponding *lacZ* fusion, whereas substitution of those marked with a green square did not. The peripheral loop (positions 87–89) and other highly divergent residues are marked with a blue triangle.

C80→A, U79→A, C75→G or 'tight stem'). The β-galactosidase activity was 1.0 MU at both 30 and 37°C.

Similar results at 30°C were also obtained with *B.japonicum* cells in which the G83→A and G83Δ fusions were integrated into the chromosome. Elimination of the bulged G83 residue resulted in enhanced repression at 30°C (Fig. 5). The mutational analyses clearly demonstrate that the degree of base pairing in the 3′-end of ROSE is an important parameter in temperature regulation.

### Additional stem–loops contribute to repression by ROSE

Derepression of the $_{58}$TCCG$_{61}$→GAAT and the C59→T mutations indicated that additional regions in ROSE$_1$ might be critical for full repression at 30°C (Fig. 2B). This segment is not highly conserved among ROSE sequences (19). Interestingly, it presents the top of a central stem–loop structure in ROSE$_1$ (Fig. 1A). The GAAT exchange at residues 58–61, which abolishes base pairing, resulted in a 40-fold increase in β-galactosidase activity at 30°C (Fig. 6). Repression was regained when base pairing was restored by the introduction of compensatory mutations in region 50–53. Hence, not the sequence but stem–loop formation in that region of ROSE$_1$ seems to be required for repression. Interestingly, the high β-galactosidase activity caused by the mutation $_{58}$TCCG$_{61}$→GAAT was not reflected in a significantly elevated transcript level (Fig. 3, compare lane 6 with lanes 2 and 7). This might indicate that presently unknown control mechanisms modulate the functionality of individual ROSE elements (see Discussion).

In addition, the mutagenesis of this potential stem–loop region provides experimental evidence that the secondary structure presented in Figure 1A might be the actual *in vivo* structure, because nucleotides 50–53 are only paired with 58–61 in that structure and not in several alternative structures (data not shown).

## DISCUSSION

Expression of sHsps and of other ROSE-controlled genes in rhizobia is tightly regulated in a temperature-dependent manner (17–19). In this study, the most important region for repression at physiological growth temperatures was mapped to the 3′-end of this negatively *cis*-acting 5′-UTR. The critical region includes the ribosome-binding site (RBS) and the AUG start codon. Incidentally, this region is highly conserved in all 15 known elements (19). Secondary structure predictions strongly suggested that the corresponding mRNA has the potential to form a stem–loop structure. RNA secondary structures are known to regulate various cellular functions such as mRNA turnover (26–28) and translation efficiency (29–31).

The involvement of the SD region and the translation start codon in base pairing implies that stem–loop formation in ROSE mRNA controls the efficiency of translation. Such a mechanism is reminiscent of the one previously proposed for the *rpoH* mRNA of *E.coli* (31,32). The secondary structure formed by this mRNA is believed to be temperature responsive. Mutagenesis studies showed a strong inverse correlation between thermostability of the *rpoH* mRNA structure and expression of *rpoH–lacZ* fusions. Part of the RBS is masked by base pairing with a so-called region B, restricting ribosome entry under non-stress conditions. Melting of the structure upon temperature up-shift presumably allows ribosome binding and promotes synthesis of the σ factor.

The model we propose also suggests two alternative conformations for the 3′-end of ROSE mRNA. At normal growth temperature, the mRNA would form a secondary structure that occludes the SD sequence and the translation initiation codon and thereby prevents ribosome access (Fig. 7). Upon heat shock, this structure would melt and enable ribosome loading and translation initiation. To this point, the model is similar to that proposed for *rpoH*. In contrast to the latter, we find only negligible amounts of ROSE-containing transcripts at normal temperature despite the constitutive character of the preceding promoter (constitutive expression at 30°C is observed with internal deletions or base substitutions in ROSE without altering the promoter sequence). This prompts us to speculate further that the secondary structure might not only confer translational control but also stability control to ROSE mRNA. Ribosome binding has been demonstrated in several cases to result in protection against ribonucleolytic degradation (33,34). In fact, ribosome protection is one of the prevailing theories established to model prokaryotic mRNA decay (35).

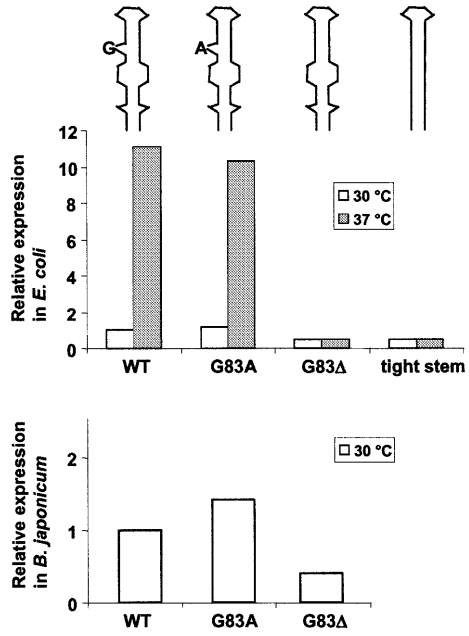


**Figure 5.** Expression of $ROSE_1$–*hspA*–*lacZ* variants with enhanced repression capacity. The different ROSE variants are illustrated schematically at the top of the figure. For details of the ROSE mutations, see Table 2. *E.coli* or *B.japonicum* cells were grown to exponential growth phase at the temperatures indicated. The β-galactosidase activity relative to the activity of the wild-type fusion at 30°C is denoted.

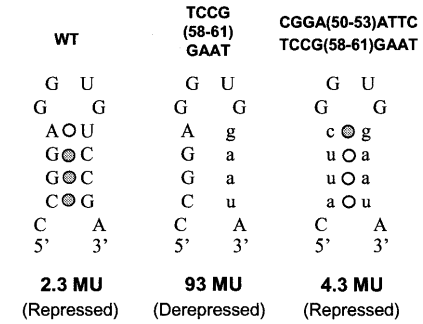


**Figure 6.** Effect of mutations in the central region of $ROSE_1$ on mRNA folding and expression. Wild-type (WT) and mutated sequences from residue 49 to 62 are shown. Mutated residues are represented by lower case letters. White circles symbolize base pairing through two hydrogen bonds, grey circles demonstrate base pairing through three hydrogen bonds. The β-galactosidase activities are given in MU.

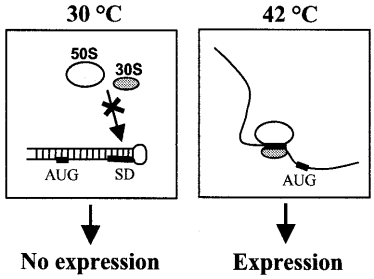


**Figure 7.** Model for temperature-responsive regulation by ROSE. The SD sequence and the AUG start codon are indicated in the schematic hairpin structure at the 3′-end of ROSE. Grey ovals represent large (50S) and small (30S) ribosomal subunits. See text for further details.

Although a ROSE-binding repressor protein can still not be ruled out as an additional layer of control, the fact that the mutational effects on ROSE-dependent expression in *B.japonicum* and *E.coli* were very similar (Fig. 2B and C) argues for a factor-independent mechanism. Moreover, the ribosome protection model alone is sufficient to explain all observations that were made during our investigation. We found that single nucleotide exchanges in ROSE permit constitutive expression at otherwise repressing temperatures. Strikingly, all mutations leading to derepression were found in predicted stem regions whereas the exchange of nucleotides in loop regions did not have any effect. Derepressed β-galactosidase values in $_{81}TT_{82}\rightarrow CA$ and C84→A at 30°C coincided with elevated transcript levels. In both ROSE variants nucleotides complementary to the SD sequence are exchanged (Fig. 4). According to our model, the RBS would be accessible in the mutated elements. This would allow ribosome entry coupled with translation initiation and mRNA protection, explaining both the elevated transcript and protein levels.

An interesting observation in this context is that the central base pair of the final secondary structure in $ROSE_1$, a C at position 77 and a G at position 99 (Fig. 4), is also present in all other characterized ROSE elements with one notable exception (Fig. 1E). In $ROSE_{N1}$ there is an A and a T, respectively, at the equivalent positions. The fact that these exchanges sustain base pairing (Fig. 1B) is strongly indicative of a requirement for mRNA folding in ROSE-mediated regulation.

The ribosome protection model predicts that the fate of ROSE-containing transcripts solely depends on the ambient temperature and that the ROSE mRNA acts as a direct thermosensor. It is easy to imagine that imperfect base pairing is necessary to guarantee melting within the appropriate temperature range. This range is rather narrow because sHsps can be induced by a shift from 30 to 37°C (18). Internal loop regions and the highly conserved bulged G (at position 83 in $ROSE_1$) opposite the SD sequence might facilitate temperature-mediated melting of ROSE mRNA. Consistent with our model, removal of the bulged G83 alone strengthened repression by $ROSE_1$. Additional improvements in the stem by introduction of paired nucleotides in internal loop regions (the 'tight stem') did not further enhance repression. In both constructs, derepression was not achieved at 37°C. Monitoring β-galactosidase activity at higher temperatures (40 or 42°C) was not possible because the enzyme is unstable under these conditions.

Post-transcriptional regulation is also in agreement with previous results. A *B.japonicum* strain carrying a translational $ROSE_1^{WT}$–*hspA*–*lacZ* fusion is known to yield only very low basal β-galactosidase activity at 30°C (17), consistent with small amounts of mRNA as determined by primer extension analysis (Fig. 3, lane 2). This result is clearly compatible with the concept that the 3′-half of ROSE forms a stem–loop structure impeding ribosome access and thereby promoting mRNA degradation. Any mutation that weakens or abolishes the

secondary structure would be expected to result in mRNA protection and derepression of $ROSE_1$–*hspA* expression. This is the case for internal deletions (Δ2–74 and Δ50–74) in ROSE, which eliminate the central stem–loop (residues 44–68) together with the region complementary to the translation start site (Fig. 1A). As base pairing opposite the SD sequence is rather weak due to the bulged G at position 83, the entire structure in the 3′-end might not be stable without its basal part and the preceding stem–loop. The assumption that additional regions might serve as a 'zipper' to facilitate formation of the proper secondary structure at the 3′-end of ROSE is strongly supported by the mutagenesis of region 58–61 in $ROSE_1$ (Fig. 6). Most likely, the actual requirements for mRNA folding are complex and might vary between individual ROSE elements as the region upstream of the strictly conserved hairpin at the 3′-end is variable not only in sequence but also in secondary structure (Fig. 1) (19). It seems plausible that the highly conserved 3′-end of ROSE is involved in direct sensing and responding to elevated temperatures. Other regions in the extended 5′-UTR might permit fine tuning of heat shock gene expression. Different induction kinetics for several ROSE-controlled sHsps support this assumption (36). The establishment of the new working model for ROSE-mediated regulation paves the way for future studies to refine our hypothesis. Already it appears that ROSE can be added to the emerging list of direct thermosensors.

## ACKNOWLEDGEMENTS

We are grateful to Hans-Martin Fischer for helpful discussions throughout the project. This study was supported by a grant from the Swiss Federal Institute of Technology, Zürich.

## REFERENCES

1. Gross,C.A. (1996) Function and regulation of the heat shock proteins. In Neidhardt,F.C. (ed.), *Escherichia coli and Salmonella*: *Cellular and Molecular Biology*. ASM Press, Washington, DC, pp. 1382–1399.
2. Yura,T., Kanemori,M. and Morita,M.T. (2000) The heat shock response: regulation and function. In Storz,G. and Hengge-Aronis,R. (eds), *Bacterial Stress Responses*. ASM Press, Washington, DC, pp. 3–18.
3. Yura,T. and Nakahigashi,K. (1999) Regulation of the heat-shock response. *Curr. Opin. Microbiol.*, **2**, 153–158.
4. Narberhaus,F. (1999) Negative regulation of bacterial heat shock genes. *Mol. Microbiol.*, **31**, 1–8.
5. Zuber,U. and Schumann,W. (1994) CIRCE, a novel heat shock element involved in regulation of heat shock operon *dnaK* of *Bacillus subtilis*. *J. Bacteriol.*, **176**, 1359–1363.
6. Hecker,M., Schumann,W. and Völker,U. (1996) Heat-shock and general stress response in *Bacillus subtilis*. *Mol. Microbiol.*, **19**, 417–428.
7. Segal,G. and Ron,E.Z. (1996) Regulation and organization of the *groE* and *dnaK* operons in Eubacteria. *FEMS Microbiol. Lett.*, **138**, 1–10.
8. Roberts,R.C., Toochinda,C., Avedissian,M., Baldini,R.L., Gomes,S.L. and Shapiro,L. (1996) Identification of a *Caulobacter crescentus* operon encoding *hrcA*, involved in negatively regulating heat-inducible transcription and the chaperone gene *grpE*. *J. Bacteriol.*, **178**, 1829–1841.
9. Yuan,G. and Wong,S.L. (1995) Regulation of *groE* expression in *Bacillus subtilis*: the involvement of the $\sigma^A$-like promoter and the roles of the inverted repeat sequence (CIRCE). *J. Bacteriol.*, **177**, 5427–5433.
10. Homuth,G., Mogk,A. and Schumann,W. (1999) Post-transcriptional regulation of the *Bacillus subtilis dnaK* operon. *Mol. Microbiol.*, **32**, 1183–1197.
11. Babst,M., Hennecke,H. and Fischer,H.M. (1996) Two different mechanisms are involved in the heat-shock regulation of chaperonin gene expression in *Bradyrhizobium japonicum*. *Mol. Microbiol.*, **19**, 827–839.
12. Mogk,A., Homuth,G., Scholz,C., Kim,L., Schmid,F.X. and Schumann,W. (1997) The GroE chaperonin machine is a major modulator of the CIRCE heat shock regulon of *Bacillus subtilis*. *EMBO J.*, **16**, 4579–4590.
13. Servant,P. and Mazodier,P. (2001) Negative regulation of the heat shock response in *Streptomyces*. *Arch. Microbiol.*, **176**, 237–242.
14. Servant,P., Grandvalet,C. and Mazodier,P. (2000) The RheA repressor is the thermosensor of the HSP18 heat shock response of *Streptomyces albus*. *Proc. Natl Acad. Sci. USA*, **97**, 3538–3543.
15. Narberhaus,F., Krummenacher,P., Fischer,H.M. and Hennecke,H. (1997) Three disparately regulated genes for $\sigma^{32}$-like transcription factors in *Bradyrhizobium japonicum*. *Mol. Microbiol.*, **24**, 93–104.
16. Minder,A.C., Fischer,H.M., Hennecke,H. and Narberhaus,F. (2000) Role of HrcA and CIRCE in the heat shock regulatory network of *Bradyrhizobium japonicum*. *J. Bacteriol.*, **182**, 14–22.
17. Narberhaus,F., Käser,R., Nocker,A. and Hennecke,H. (1998) A novel DNA element that controls bacterial heat shock gene expression. *Mol. Microbiol.*, **28**, 315–323.
18. Münchbach,M., Nocker,A. and Narberhaus,F. (1999) Multiple small heat shock proteins in rhizobia. *J. Bacteriol.*, **181**, 83–90.
19. Nocker,A., Krstulovic,P., Perret,X. and Narberhaus,F. (2001) ROSE elements occur in disparate rhizobia and are functionally interchangeable between species. *Arch. Microbiol.*, **176**, 44–51.
20. Regensburger,B. and Hennecke,H. (1983) RNA polymerase from *Rhizobium japonicum*. *Arch. Microbiol.*, **135**, 103–109.
21. Sambrook,J.E., Fritsch,F. and Maniatis,T. (1989) *Molecular Cloning: A Laboratory Manual*, 2nd Edn. Cold Spring Harbor Laboratory Press, Cold Spring Harbor, NY.
22. Thompson,J.D., Higgins,D.G. and Gibson,T.J. (1994) CLUSTAL W: improving the sensitivity of progressive multiple sequence alignment through sequence weighting, positions-specific gap penalties and weight matrix choice. *Nucleic Acids Res.*, **22**, 4673–4680.
23. Zuker,M., Mathews,D.H. and Turner,D.H. (1999) Algorithms and thermodynamics for RNA secondary structure prediction: a practical guide. In Barciszewski,J. and Clark,B.F.C. (eds), *RNA Biochemistry and Biotechnology*. Kluwer Academic, Dordrecht, The Netherlands, pp. 11–43.
24. Simon,R., Priefer,U. and Pühler,A. (1983) Vector plasmids for *in vivo* and *in vitro* manipulation of Gram-negative bacteria. In Pühler,A. (ed.), *Molecular Genetics of the Bacteria–Plant Interaction*. Springer Verlag, Heidelberg, Germany, pp. 98–106.
25. Imai,Y., Matsushima,Y., Sugimura,T. and Terada,M. (1991) A simple and rapid method for generating a deletion by PCR. *Nucleic Acids Res.*, **19**, 2785.
26. Régnier,P. and Arraiano,C.M. (2000) Degradation of mRNA in bacteria: emergence of ubiquitous features. *Bioessays*, **22**, 235–244.
27. Andersen,P.E. and Gober,J.W. (2000) FlbT, the post-transcriptional regulator of flagellin synthesis in *Caulobacter crescentus*, interacts with the 5′ untranslated region of flagellin mRNA. *Mol. Microbiol.*, **38**, 41–51.
28. Hambraeus,G., Persson,M. and Rutberg,B. (2000) The *aprE* leader is a determinant of extreme mRNA stability in *Bacillus subtilis*. *Microbiology*, **146**, 3051–3059.
29. de Smit,M.H. and van Duin,J. (1990) Secondary structure of the ribosome binding site determines translational efficiency: a quantitative analysis. *Proc. Natl Acad. Sci. USA*, **87**, 7668–7672.
30. de Smit,M.H. and van Duin,J. (1993) Translational initiation at the coat-protein gene of phage MS2: native upstream RNA relieves inhibition by local secondary structure. *Mol. Microbiol.*, **9**, 1079–1088.
31. Morita,M., Kanemori,M., Yanagi,H. and Yura,T. (1999) Heat-induced synthesis of $\sigma^{32}$ in *Escherichia coli*: structural and functional dissection of *rpoH* mRNA secondary structure. *J. Bacteriol.*, **181**, 401–410.
32. Morita,M.T., Tanaka,Y., Kodama,T.S., Kyogoku,Y., Yanagi,H. and Yura,T. (1999) Translational induction of heat shock transcription factor $\sigma^{32}$: evidence for a built-in RNA thermosensor. *Genes Dev.*, **13**, 655–665.
33. Braun,F., Le Derout,J. and Régnier,P. (1998) Ribosomes inhibit RNase E cleavage which induces the decay of the *rpsO* mRNA of *Escherichia coli*. *EMBO J.*, **17**, 4790–4797.
34. Iost,I. and Dreyfus,M. (1995) The stability of *Escherichia coli lacZ* mRNA depends upon the simultaneity of its synthesis and translation. *EMBO J.*, **14**, 3252–3261.
35. Carrier,T.A. and Keasling,J.D. (1997) Mechanistic modeling of prokaryotic mRNA decay. *J. Theor. Biol.*, **189**, 195–209.
36. Münchbach,M., Dainese,P., Staudenmann,W., Narberhaus,F. and James,P. (1999) Proteome analysis of heat shock protein expression in *Bradyrhizobium japonicum*. *Eur. J. Biochem.*, **264**, 39–48.